

The GEO 600 gravitational wave detector

**B Willke^{1,3}, P Aufmuth¹, C Aulbert⁴, S Babak⁵, R Balasubramanian⁵,
B W Barr², S Berukoff⁴, S Bose⁴, G Cagnoli², M M Casey²,
D Churches⁵, D Clubley², C N Colacino¹, D R M Crooks², C Cutler⁴,
K Danzmann^{1,3}, R Davies⁵, R Dupuis², E Elliffe², C Fallnich⁶,
A Freise³, S Goßler¹, A Grant², H Grote³, G Heinzel¹, A Heptonstall²,
M Heurs¹, M Hewitson², J Hough², O Jennrich², K Kawabe³, K Kötter¹,
V Leonhardt¹, H Lück^{1,3}, M Malec¹, P W McNamara², S A McIntosh²,
K Mossavi³, S Mohanty⁴, S Mukherjee⁴, S Nagano², G P Newton²,
B J Owen⁴, D Palmer², M A Papa⁴, M V Plissi², V Quetschke¹,
D I Robertson², N A Robertson², S Rowan², A Rüdiger³,
B S Sathyaprakash⁵, R Schilling³, B F Schutz^{4,5}, R Senior⁵,
A M Sintes⁴, K D Skeldon², P Sneddon², F Stief¹, K A Strain²,
I Taylor⁵, C I Torrie², A Vecchio^{4,7}, H Ward², U Weiland¹, H Welling⁶,
P Williams⁴, W Winkler³, G Woan² and I Zawischa⁶**

¹ Institut für Atom- und Molekülphysik, Universität Hannover, Callinstr. 38, 30167 Hannover, Germany

² Physics & Astronomy, University of Glasgow, Glasgow G12 8QQ, UK

³ Max-Planck-Institut für Gravitationsphysik, Albert-Einstein-Institut, Außenstelle Hannover, Callinstr. 38, 30167 Hannover, Germany

⁴ Max-Planck-Institut für Gravitationsphysik, Albert-Einstein-Institut, Am Mühlenberg 1, 14476 Golm, Germany

⁵ Department of Physics and Astronomy, Cardiff University, PO Box 913, Cardiff, CF2 3YB, UK

⁶ Laser Zentrum Hannover e. V., Hollerithallee 8, 30419 Hannover, Germany

⁷ School of Physics and Astronomy, The University of Birmingham, Edgbaston, Birmingham, B15 2TT, UK

Received 2 October 2001, in final form 14 November 2001

Published 11 March 2002

Online at stacks.iop.org/CQG/19/1377

Abstract

The GEO 600 laser interferometer with 600 m armlength is part of a worldwide network of gravitational wave detectors. Due to the use of advanced technologies like multiple pendulum suspensions with a monolithic last stage and signal recycling, the anticipated sensitivity of GEO 600 is close to the initial sensitivity of detectors with several kilometres armlength. This paper describes the subsystems of GEO 600, the status of the detector by September 2001 and the plans towards the first science run.

PACS number: 0480N

(Some figures in this article are in colour only in the electronic version)

1. Introduction

An international network of earth-bound laser-interferometric gravitational wave detectors is currently in the final commissioning phase. These detectors will be searching for gravitational waves from a number of different astrophysical sources like supernovae explosions, non-symmetric pulsars, inspiralling binary systems of neutron stars or black holes and remnants of the big bang. Furthermore, unknown sources may produce gravitational waves of detectable strength. A summary of the current understanding of astrophysical sources for gravitational waves and of predicted event rates is given in [1]. Although the expected sensitivities of the detectors under construction might be high enough to detect the first gravitational waves, only future detector generations with advanced technologies promise an event rate suitable for gravitational wave astronomy.

Six laser interferometric gravitational wave detectors are currently under construction: three interferometers of the LIGO project [2] in the USA (two interferometers with 4 km baseline and one interferometer with 2 km baseline), one detector of the French–Italian VIRGO project [3] in Italy with 3 km baseline, the TAMA detector [4] in Japan with a baseline of 300 m and the British–German GEO 600 detector with 600 m armlength in Germany. An 80 m prototype interferometer with the option to extend it to a large-scale detector is under construction by the ACIGA project in Australia [5].

The GEO 600 detector was designed based on the experience with two prototypes: the 10 m interferometer at the Glasgow University and the 30 m interferometer at the Max-Planck-Institut für Quantenoptik in Garching, near Munich. The construction of GEO 600 started in 1995 as a German/British collaboration on a site near Hannover in Germany and will be completed in 2002. Based on the constraint that the length of the vacuum pipes could not exceed 600 m, an advanced optical layout including signal recycling and novel techniques for the seismic isolation systems were included in the detector design. In parallel to the commissioning of the detector methods for data analysis as well as simulations of possible sources were developed at the University of Cardiff and at the Albert-Einstein-Institut of the Max-Planck-Gesellschaft in Potsdam.

The following sections of this paper will describe the different subsystems of the GEO 600 detector, briefly review the detector characterization and data analysis effort within GEO 600 and end with an outline of the future plans.

2. Noise sources and design sensitivity

The measured quantity in a laser interferometric gravitational wave detector is the change of the light power on a photodetector placed at the interferometer output. A fluctuation of the light power at this photodetector can be caused by many different sources. A gravitational wave passing through the detector plane causes the light beams to accumulate a phase difference $\delta\varphi_{\text{gw}}$ while travelling through the interferometer arms, and the signature of the gravitational wave can be detected as a power modulation δI_{gw} on the photodetector. A change δI_{noise} of that light power can as well be due to laser power fluctuations of either technical or quantum nature or a displacement of the mirrors caused by seismic motion or thermal noise. Some of the numerous additional noise sources that have to be taken into account are fluctuations of the index of refraction on the optical path, laser frequency fluctuations in combination with a difference in the arm length of the interferometer and coherent superposition of the main laser beam with light scattered from optical components.

To describe the sensitivity of a gravitational wave detector a quantity h is defined as: $h = \Delta L/\ell$. In this equation ℓ is the optical path length of one interferometer arm and ΔL is

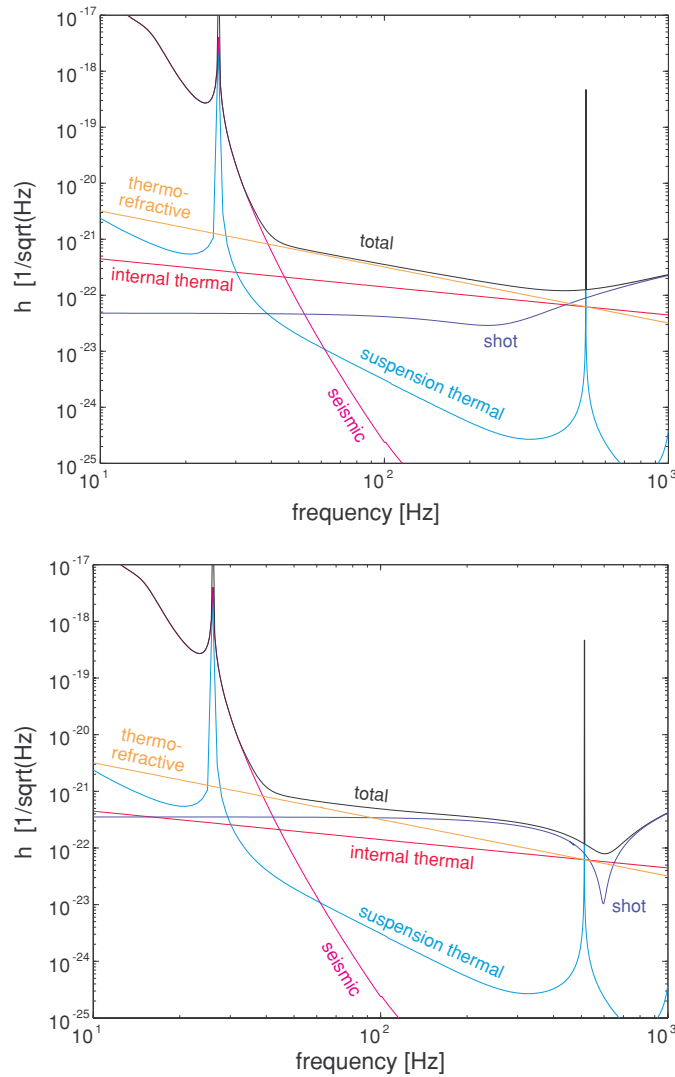


Figure 1. Expected noise spectral density of the GEO 600 detector shown in two different modes of operation: broad-band (upper) and narrow-band (lower).

the apparent differential change in optical path length between the two interferometer arms, which is either caused by a gravitational wave or by a noise process. We call it apparent length change as it can be due to either a real displacement of a mirror or to a different process changing the phase of the light when it returns to the beamsplitter. To be able to quantitatively describe noise sources like laser power noise on the photodetector that do not directly change the phase of the two interfering beams we calculate the ΔL which would cause the same power modulation on the output photodetector. By this method h can be used to describe all noise sources of a detector as well as the signal strength of a gravitational wave. As some of the noise sources have a very strong frequency dependence, the spectral density \tilde{h}_{noise} is widely used to describe the so-called strain sensitivity of laser-interferometric gravitational-wave detectors.

Three main noise sources will limit the expected sensitivity of the GEO 600 detector as shown in figure 1. The low-frequency range below 40 Hz will be limited by seismic noise.

In the intermediate region thermo-refractive noise [6] will be the main contribution and shot noise on the interferometer-output photodetector will dominate the noise spectral density in the high Fourier frequency range. The expected thermal noise of the mirror and the suspension are plotted as well. Other noise sources such as radiation pressure noise, residual gas fluctuations, gravity gradient noise or laser noise are omitted in this figure as they are not expected to limit the performance of GEO 600.

One feature of figure 1 is special for GEO 600, which is the shape of the shot-noise curve. The use of the signal-recycling technique [7] allows shaping of the shot-noise curve in the strain-sensitivity plot. By changing the reflectivity and position of the signal-recycling mirror the bandwidth and the centre frequency of the dip in the shot-noise curve can be tuned. The left part of figure 1 shows the broad-band case, and in the right part the expected shot noise for narrow-band signal recycling tuned to 600 Hz is plotted.

3. Buildings and vacuum system

To avoid fluctuations of the optical path length caused by a fluctuating index of refraction, the whole interferometer has to be set up in a high-vacuum system. For this purpose GEO 600 uses two 600 m long vacuum tubes of 60 cm diameter which are suspended in a trench in the ground. A novel convoluted-tube design which allows a wall thickness of only 0.8 mm was used to reduce the weight and cost of the stainless-steel vacuum tube. Baffles were installed inside the tube to avoid stray light reflections by the shiny tube wall. Each tube was baked for two days in air at 200 °C and for one week under vacuum at 250 °C. Currently the pressure in the beam tubes is in the upper 10^{-9} mbar region.

One central building (13 m × 8 m in size) and two end buildings (6 m × 3 m) accommodate the vacuum tanks (2 m tall) in which the optical components are suspended. Eight of these tanks form a cluster in the central building which can be subdivided into three sections to allow mirror installation without venting the whole cluster. Therefore only short down-times are expected for a change of the signal-recycling mirror, needed to change the detector bandwidth.

The whole vacuum system, except for the modecleaner section, is pumped by four magnetically levitated turbo pumps with a pumping speed of 1000 l s^{-1} , each backed by a scroll pump ($25 \text{ m}^3 \text{ h}^{-1}$). Additional dedicated pumping systems are used for the modecleaner and the signal-recycling section.

Great care was taken to minimize contamination of the vacuum system by hydrocarbons. For this reason the seismic isolation stacks, which comprise rubber and other materials containing hydrocarbons, are sealed by bellows and pumped separately. Furthermore, the light-emitting diodes (LEDs), the photodiodes and the feedback coils used as sensors and actuators in the pendulum damping systems are sealed in glass encapsulations.

The buildings of GEO 600 are split into three regions with different cleanroom classes: the so-called gallery where people can visit and staff can work with normal clothes, the inner section which has a cleanroom class of 1000 and a movable cleanroom tent installed over open tanks with a cleanroom class 100.

4. Seismic isolation and thermal noise

One of the most important sub-systems in a laser-interferometric gravitational-wave detector is the seismic isolation and suspension system. The spectral density of the seismic ground motion at the GEO site is about eight orders of magnitude above the displacement requirement for the mirror. The filter effect of a sequential system of harmonic oscillators with resonance frequencies below 10 Hz is used to isolate the mirrors against this seismic motion.

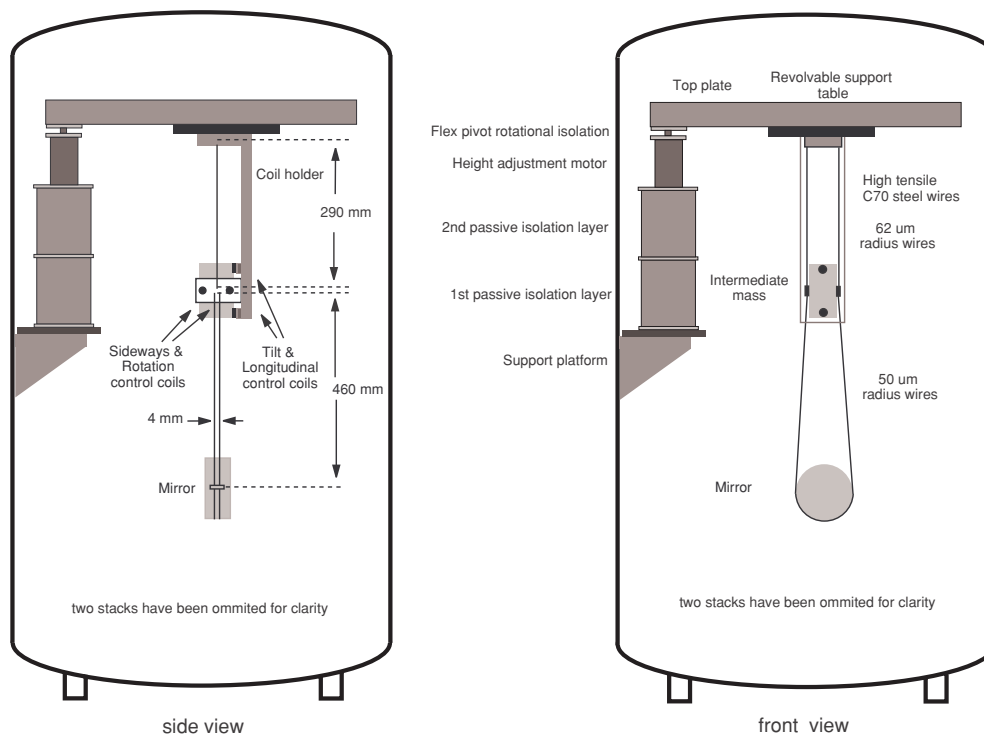


Figure 2. The GEO 600 modecleaner suspension system. Two passive stack layers, a rotational flexure and a double pendulum are used to isolate the modecleaner mirror from seismic noise. The quality factor of a violin mode of this suspension at 190 Hz was measured to be between 5×10^5 and 1×10^6 .

Two different types of isolation systems are implemented in GEO 600. The first one, which is used to isolate the modecleaner optics, consists of a top plate supported by three legs and a double-pendulum suspension (see figure 2). Each leg has two passive isolation layers (rubber layers with an intermediate stainless-steel mass) which are followed by horizontal adjustment motors and flex-pivot rotation springs to reduce rotational coupling between the vacuum tank and the top plate. To avoid an excitation of the pendulum mode four co-located control systems measure the motion of the intermediate mass with respect to a coil-holder arm that is rigidly attached to the top plate. These so-called local controls use shadow sensors and feedback coils that apply forces to magnets glued to the intermediate mass. The bandwidth of these local controls is about 3 Hz. The intermediate mass is suspended by two wires and the modecleaner mirrors are supported by two wire slings. These mirrors are 10 cm in diameter and 5 cm thick. This arrangement allows us to control tilt and rotation of the mirror as well as its sideways and longitudinal position at the intermediate-mass level. Hence the coil/magnet units of the local controls can also be used for automatic alignment control of the modecleaners [8]. Small fused-silica prisms are attached to the mirrors to define the break-off points of the wires from the mirror circumference. A fixed break-off point reduces the friction of the wire on the mirror which directly affects the thermal noise. A measurement of the quality factor Q of the violin modes of the modecleaner suspensions shows Q values between 5×10^5 and 1×10^6 . To allow fast feedback of the modecleaner length-control system, a second double pendulum called a reaction pendulum is placed a few millimetres behind one mirror of each modecleaner. The bottom mass of the reaction pendulum carries coils which act on magnets

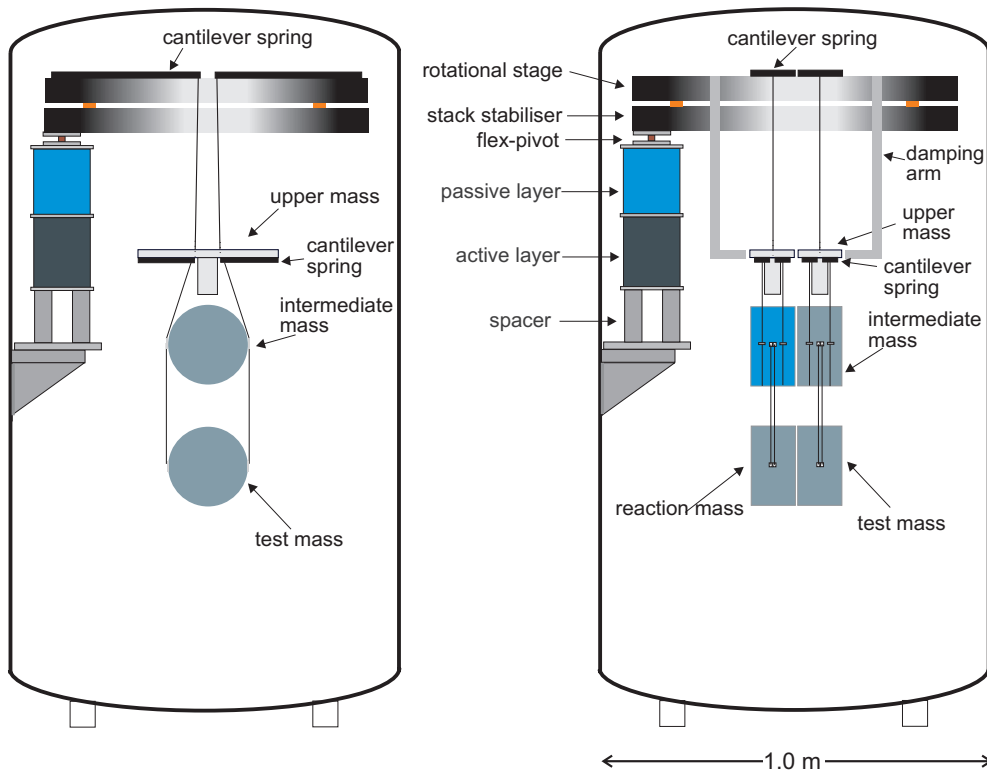


Figure 3. The GEO 600 main suspension system. Two stack layers (one active, one passive), a rotational flexure, two vertical cantilever stages and a triple horizontal pendulum are used to isolate the test mass from seismic noise. The lower pendulum stage is a monolithic fused-silica design to minimize thermal noise.

glued to the corresponding mirror. This provides a feedback actuator with small seismic motion above 10 Hz Fourier frequency.

Figure 3 shows the seismic isolation system used to isolate the beam splitter and the mirrors of the Michelson interferometer. Just as for the modecleaner suspensions three legs support the so-called stack stabilizer and the rotational stage. Without lateral movement the rotational stage can be rotated with respect to the stack stabilizer to allow for rotational pre-alignment of the mirror. The mirror is the lowest mass of a triple pendulum with two blade-spring stages for vertical isolation which is mounted to the rotational stage. Each leg has an active and a passive layer for seismic isolation. The active system consists of three 2 Hz geophones to sense the motion of the upper plate of a three-axis piezo actuator. By means of a feed-forward control system for the horizontal and a feedback system for the vertical direction the motion of this upper plate is reduced with respect to the seismic ground motion. On top of this plate a rubber/stainless-steel isolation layer is placed, and a flex-pivot is used for rotational isolation.

The triple pendulum has three masses: an upper mass made of stainless steel, a fused-silica intermediate mass and the mirror which is 18 cm in diameter (the beam splitter diameter is 26 cm). In the case of the triple pendulum six co-located feedback systems are used to damp all degrees of freedom of the upper mass. Due to the specific design of the triple pendulum this damping extracts energy from all pendulum modes below Fourier frequencies of 10 Hz. Similar to the modecleaner suspension the coil-magnet units of these local controls are used

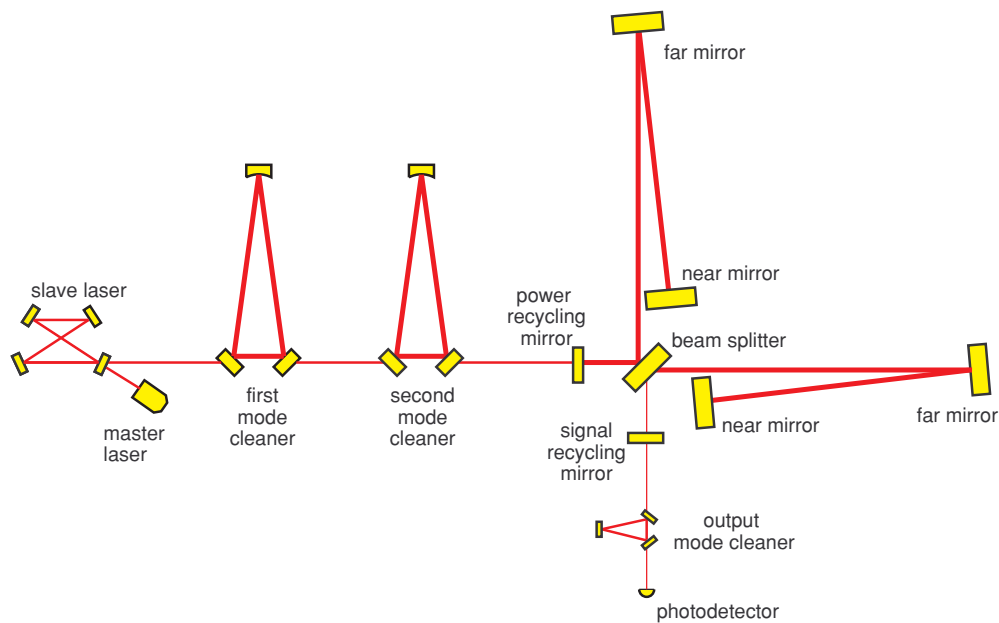


Figure 4. Optical layout of GEO 600: a 12 W injection-locked laser system is filtered by two sequential modecleaners and injected into the dual-recycled interferometer. A folded light path is used to increase the round-trip length of the interferometer arms to 2400 m. An output modecleaner will be used to spatially clean the laser mode before it reaches the photodetector.

as actuators for the automatic alignment-control systems. The reaction pendulums for length control of the Michelson interferometer consist of similar triple pendulums suspended 3 mm behind the corresponding mirror. The intermediate mass of the reaction pendulum carries coils that act on mirrors glued to the intermediate mass of the mirror triple pendulum. To keep the internal quality factor of the mirrors as high as possible no magnets are glued to the mirror itself but electrostatic feedback between the mirror and the lowest mass of the reaction pendulum is used to apply feedback forces in the high Fourier frequency range. A detailed description of the seismic isolation system can be found in the paper of Plissi *et al* [9].

To minimize the internal thermal noise of the mirror and the pendulum thermal noise, the lowest pendulum stage is made entirely from fused silica. The Q of fused-silica suspensions of comparable size has been demonstrated to be as high as 1×10^7 [10]. Small fused-silica pieces are attached to the intermediate mass and to the mirror itself by a technique called hydroxide-catalysis bonding [11]. This technique provides high-strength bonds and allows the quality factors to be kept high and thus the thermal noise low. Four fused-silica fibres with $270 \mu\text{m}$ diameter are welded to these fused-silica pieces and support the mirrors.

5. Optical layout

The optical layout of GEO 600 (see figure 4) has three major parts: the laser system, two sequential input modecleaners and the dual-recycled Michelson interferometer with the output modecleaner and the main photodetector at its output port. Some steering mirrors, electro-optical modulators and Faraday isolators are omitted in figure 4. All optical components except the laser system and the photodetector are suspended inside the vacuum system.

5.1. Laser system and modecleaners

The GEO 600 laser system is based on an injection-locked laser-diode-pumped Nd:YAG system with an output power of 12 W. A non-planar ring-oscillator (NPRO) with an output power of 0.8 W is used as the master laser.

Two Nd:YAG crystals, each pumped by a fibre-coupled laser diode with a power of 17 W, are used as the active medium in the four-mirror slave ring cavity. Three of these mirrors and a piezo-electric transducer (PZT) carrying the fourth mirror are mounted on a rigid invar spacer to increase the mechanical stability of the slave-laser cavity. A measurement of the free-running frequency noise of the slave laser showed that the fluctuations in the acoustic Fourier frequency range are of an order of magnitude lower for the rigid spacer design than compared to a slave cavity with discrete mirror mounts. The PZT is used to control the length of the 45 cm long resonator to keep the slave-laser frequency within the injection-locking range of 1.6 MHz. Two Brewster plates are incorporated in the slave cavity to define the polarization direction, reduce depolarization losses and compensate for the astigmatism introduced by the curved mirrors of the slave resonator. The good spatial beam quality ($M^2 \leq 1.05$) of the injection-locked laser system allowed us to couple 95% of the light into a Fabry–Perot resonator. The frequency noise of the injection-locked laser system was measured to be dominated by the master-laser frequency fluctuations. The free-running intensity noise which is in the $10^{-6} \text{ Hz}^{-1/2}$ region for Fourier frequencies between 10 Hz and 1 kHz is dominated by fluctuations of the slave-laser pump diodes. Feeding back to these pump diodes, the relative power noise could be reduced to a level below $10^{-7} \text{ Hz}^{-1/2}$. A detailed description of the GEO 600 laser system can be found in [12].

The light from the laser system is injected into the two modecleaners, each with 8 m round-trip length. The main purpose of the two sequential modecleaners is the spatial filtering of the laser beam [13]. In the frame of the suspended interferometer even a perfect laser beam would show spatial fluctuations due to the motion of the laser table relative to the suspended interferometer. Hence the modecleaner filter cavities have to be suspended as well. The laser frequency is stabilized to the resonance frequency of the first modecleaner MC1 by feeding back to the master-laser's temperature and PZT actuator. A phase-correcting Pockels cell between the master and the slave laser is used to enhance the bandwidth of this first control loop to approximately 100 kHz.

With the first control loop in place the laser frequency will change when the length of MC1 changes. Due to this effect the length-control actuator of MC1 can be used to bring the laser/MC1 unit into resonance with the second modecleaner MC2. To increase the bandwidth of this loop the high Fourier frequency components of the control signal are fed into the error point of the first loop. A third control loop is used to bring the laser/MC1/MC2 unit into resonance with the power-recycling cavity. A detailed description of the frequency control scheme of GEO 600 is given in [14].

Under the assumption that the laser exactly follows the resonance frequency of the first modecleaner, the control signal needed to stabilize the laser/MC1 unit to the second modecleaner can be used to analyse the fluctuations between the lengths of the two modecleaners (see figure 5). Under the additional assumption that the modecleaner mirrors move independently of each other this measurement describes the motion of the modecleaner mirrors. The rms length changes of the modecleaners in time intervals of 10 s is below $1 \mu\text{m}$ which allows a lock acquisition of the modecleaners within typically 10 s.

Until now the modecleaners were only operated with an attenuated laser beam of 1 W power. With this power level 85% of the light was transmitted through the first modecleaner and approximately 500 mW were measured behind the second modecleaner. An automatic

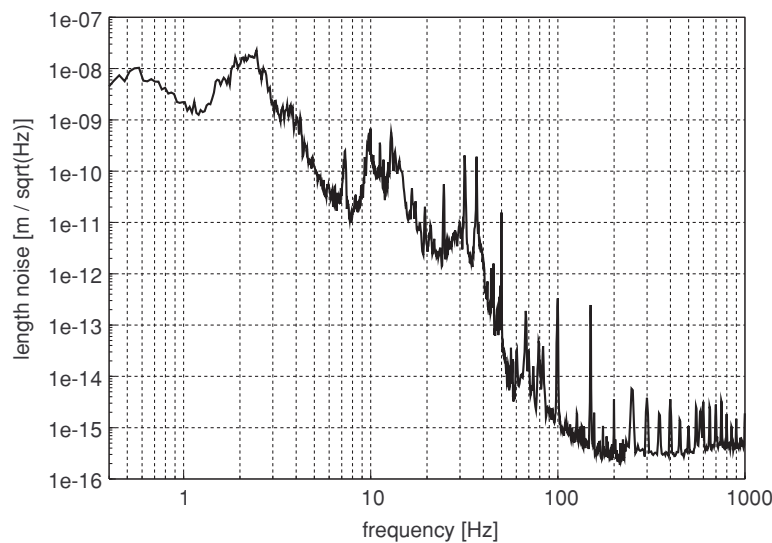


Figure 5. Displacement-noise spectral density of the GEO 600 modecleaner mirrors. For this measurement the laser was locked to the first modecleaner and the actuator signal needed to lock the second modecleaner to the stabilized laser was calibrated.

alignment and drift control system is used to maintain the alignment of the modecleaner cavities. The error signals generated by the differential-wavefront-sensing method were diagonalized to get control signals for the three different mirrors. The feedback was applied to the intermediate mass of the modecleaner double pendulums. This means that for frequencies above 1 Hz the actuator has a $1/f^4$ transfer function from the coil current to the mirror displacement. Nevertheless, a unity-gain frequency of about 10 Hz was achieved. For a detailed description of the automatic alignment system see [8]. With this automatic alignment system installed, continuous lock periods of more than 48 hours were achieved for both modecleaners.

5.2. Interferometer and recycling cavities

The main interferometer is designed as a dual-recycled folded-arm Michelson interferometer. Dual recycling on a suspended interferometer was first demonstrated by Heinzel *et al* [15]. A length-control-loop system keeps the operating point of the interferometer at the so-called dark fringe which means that due to destructive interference no light leaves the output port of the interferometer. Under this condition all light is reflected back towards the laser and the interferometer behaves like a mirror. A so-called power-recycling cavity is formed by this ‘mirror’ and the power-recycling mirror (see figure 4) which leads to a power buildup in the interferometer and improves the shot-noise-limited sensitivity of the detector. The anticipated power buildup in GEO 600 is 2000 which leads to a power of about 10 kW at the beam splitter. Any phase change of the light in the interferometer arms caused by a gravitational wave or noise will lead to light leaking out at the output port of the interferometer. The signal-recycling mirror will reflect this light back into the interferometer, thus forming another Fabry–Perot cavity: the signal-recycling cavity. In this case, the light power representing the signal at specific Fourier frequencies is enhanced. This effect reduces the shot-noise-equivalent apparent displacement noise of the detector for these Fourier frequencies. The shot-noise curve shows a dip, the centre frequency of which can be tuned by changing the position of

the signal-recycling mirror. The bandwidth of the dip is determined by the reflectivity of that mirror. Due to unequal radii of curvature of the interferometer mirrors and due to a thermal lens that develops in the beamsplitter as the power in the power-recycling cavity increases, the achieved interferometer contrast will not be perfect and some light in higher order spatial modes will leave the output port. This light could increase the shot noise on the photodetector without enhancing the signal. Even though signal recycling improves the interferometer contrast due to the ‘mode-healing’ effect [15], an output modecleaner will be implemented in GEO 600 to reduce the higher-order-mode content of the light reaching the photodetector. The photodetector consists of 16 InGaAs photodiodes of 2 mm diameter, each of which can operate up to 50 mA of photocurrent. The AC part of the photocurrent of these diodes will be combined and demodulated at the modulation frequency of the heterodyne readout scheme.

6. Detector control and data analysis

GEO 600 has four suspended cavities and the suspended Michelson interferometer all of which need length and alignment control systems. Twenty-five pendulums need local damping of at least four degrees of freedom, eight vacuum tanks have active seismic isolation control (in three supporting legs each) and additional feedback-control systems are needed for the laser stabilization. Most of these control loops are implemented with analogue electronic controllers with some guidance by a LabView computer-control environment [16]. Only the active seismic isolation and some slow alignment-drift-control systems are implemented as digital control loops. The LabView computer control has authority to allow pre-alignment, guide lock acquisition, monitor the detector status and compensate for long-term drifts. Typical response times of this system are 100 ms.

Although only the $h(t)$ channel includes a possible gravitational-wave signal, a multi-channel data acquisition system is needed to detect environmental and detector disturbances and exclude false detections. Two different sampling rates (16 384 Hz and 512 Hz) are used in the data-acquisition system of GEO 600. In the central building 32 fast channels and 64 slow channels are available, and in each of the end buildings we can use 16 fast channels. Most of these channels will be used for detector characterization only. A selection of those channels together with information coming from the LabView control program will be combined as a data stream with a data rate of approximately 0.5 MByte s^{-1} and sent via a radio link from the site to Hannover where the data will be stored. From here the data will be distributed to the data-analysis groups, whereas the time-critical data analysis will be performed in Hannover.

Due to the low signal-to-noise ratio of expected gravitational-wave signals a very good understanding of the detector noise is needed to perform an adequate data analysis. Furthermore, an extensive detector characterization effort [17] during the commissioning phase can help to identify noise sources and improve the sensitivity. Based on the understanding of the detector noise sources a so-called detector characterization robot (DCR) [18] will be developed to condition the data and provide false-alarm vetos for the data analysis.

A common analysis of the LIGO and GEO 600 data will be performed within the GEO 600 project as well as in the LIGO Scientific Community. Four different BeoWolf computer clusters will be used in the GEO 600 project for the search for gravitational waves from different sources. A cluster with 14 nodes in Hannover will perform the DCR data conditioning and the transient-data analysis. Three different BeoWolf clusters, each with more than 100 nodes, at the Albert-Einstein-Institut in Potsdam, Germany, at the Cardiff University, Great Britain and at the University of Birmingham, Great Britain will be used to search for coalescing binary systems, pulsars and unknown sources. A group at the University of Glasgow will perform the search for gravitational waves from known pulsars.

7. Current status and outlook

As mentioned above, the laser system and the two modecleaners of GEO 600 are installed and are working reliably. Stretches of continuous locking for more than 48 h were achieved. The two far mirrors of GEO 600 are installed with monolithic suspensions. To reduce the risk of contamination during the commissioning phase, test optics are currently installed for the near mirrors and the beamsplitter. With this configuration an interference contrast of better than 99% was measured. With the help of an automatic gain-control electronic circuit we were able to lock the power-recycling cavity with the Michelson interferometer swinging through fringes, and we expect to achieve the first lock of the Michelson interferometer soon. Once the Michelson interferometer is locked we will have a first optimization phase of the detector followed by a two-week coincidence run between LIGO and GEO scheduled for the end of 2001. This coincidence run will be followed by the implementation of signal recycling in early 2002. Once the dual-recycled Michelson is working reliably we plan to replace the test optics with the final optics, enhance the circulating power and have a second optimization period. This period will be followed by the first science run.

Acknowledgments

The authors would like to thank the British Particle Physics and Astronomy Research Council (PPARC), the German Bundesministerium für Bildung und Forschung (BMBF) and the State of Lower Saxony (Germany) for their funding and continuous support of the GEO 600 project.

References

- [1] Schutz B F 1999 *Class. Quantum Grav.* **16** A131
- [2] Sigg D 2002 *Proc. of the 4th Edoardo Amaldi Conf. on Gravitational Waves (Perth, Western Australia, 8–13 July 2001)* *Class. Quantum Grav.* **19** 1429
- [3] Di Fiore L 2002 *Proc. of the 4th Edoardo Amaldi Conf. on Gravitational Waves (Perth, Western Australia, 8–13 July 2001)* *Class. Quantum Grav.* **19** 1421
- [4] Ando M 2002 *Proc. of the 4th Edoardo Amaldi Conf. on Gravitational Waves (Perth, Western Australia, 8–13 July 2001)* *Class. Quantum Grav.* **19** 1409
- [5] McClelland D 2001 Talk presented at *4th Edoardo Amaldi Conf. on Gravitational Waves (Perth, Western Australia, 8–13 July 2001)*
- [6] Wanser K H 1992 *Electron. Lett.* **28** 53
- [7] Meers B J *et al* 1988 *Phys. Rev. D* **38** 2317
- [8] Grote H *et al* 2002 *Proc. of the 4th Edoardo Amaldi Conf. on Gravitational Waves (Perth, Western Australia, 8–13 July 2001)* *Class. Quantum Grav.* **19** 1849
- [9] Plissi M V *et al* 2000 *Rev. Sci. Instrum.* **71** 2539
- [10] Cagnoli G *et al* 2000 *Phys. Rev. Lett.* **85** 2442
- [11] Rowan S *et al* 1998 *Phys. Lett. A* **246** 471
- [12] Zawischa I *et al* 2002 *Proc. of the 4th Edoardo Amaldi Conf. on Gravitational Waves (Perth, Western Australia, 8–13 July 2001)* *Class. Quantum Grav.* **19** 1775
- [13] Rüdiger A *et al* 1981 *Opt. Acta* **28** 641
- [14] Freise A *et al* 2002 *Proc. of the 4th Edoardo Amaldi Conf. on Gravitational Waves (Perth, Western Australia, 8–13 July 2001)* *Class. Quantum Grav.* **19** 1389
- [15] Heinzel G *et al* 1998 *Phys. Rev. Lett.* **81** 5493
- [16] Casey M *et al* 2000 *Rev. Sci. Instrum.* **71** 3910
- [17] Kötter K *et al* 2002 *Proc. of the 4th Edoardo Amaldi Conf. on Gravitational Waves (Perth, Western Australia, 8–13 July 2001)* *Class. Quantum Grav.* **19** 1399
- [18] Mohanty S D and Mukherjee S 2002 *Proc. of the 4th Edoardo Amaldi Conf. on Gravitational Waves (Perth, Western Australia, 8–13 July 2001)* *Class. Quantum Grav.* **19** 1471